

# Supporting Information for “Predicting the elemental geochemistry of fluvial sediments: A case study from the Cairngorms, UK”

Alex G. Lipp<sup>1</sup>, Gareth G. Roberts <sup>1</sup>, Alex Whittaker <sup>1</sup>, Charles Gowing <sup>2</sup>,

Victoria Fernandes <sup>1</sup>

<sup>1</sup>Department of Earth Sciences and Engineering, Imperial College London

<sup>2</sup>British Geological Survey, Keyworth

## Contents of this file

1. Figures S1–S24

2. Video S1

## Introduction

This document contains supplementary figures that show the results of tests in which input to the predictive geochemical model was changed and an exploration of model predictions. A time-lapse video that shows the higher-order river sediment sampling procedure is also included as additional supplementary material.

Figure S1 shows predicted concentrations of Mg downstream if substrate, which is input to the model, is changed. In the first test substrate is substituted for a section of the G-BASE dataset taken from elsewhere in the UK (arbitrarily, Wales/Herefordshire). In

the second test the G-BASE measurements from the study region are randomised before interpolation and insertion into the model. As Figures S1b and S1d show, neither approach generates accurate predictions of downstream chemistry (see coloured circles and inset panels). In contrast, using the actual geochemistry of the Cairngorms (extracted from the G-BASE dataset) generates accurate predictions (see main manuscript). These results emphasise the sensitivity of downstream geochemistry to the specific distribution of upstream geochemistry.

Figure S2 shows the global root-mean-squared (RMS) misfit for all elements in this study. RMS misfit,  $H$ , is calculated such that

$$H = \left[ \frac{1}{N} \sum_{i=1}^N \left( \log_{10} C_o^i - \log_{10} C_c^i \right)^2 \right]^{1/2}, \quad (1)$$

where  $N$  is the number of measured elemental concentrations for each sample,  $C_o$  and  $C_c$  are observed and calculated concentrations of each element ( $i$ ).

Figures S3–S24 show the misfit for each element,  $\log_{10} C_o^i - \log_{10} C_c^i$ .

Video S1 is a timelapse video demonstrating the higher-order river sediment sampling procedure used in this study.

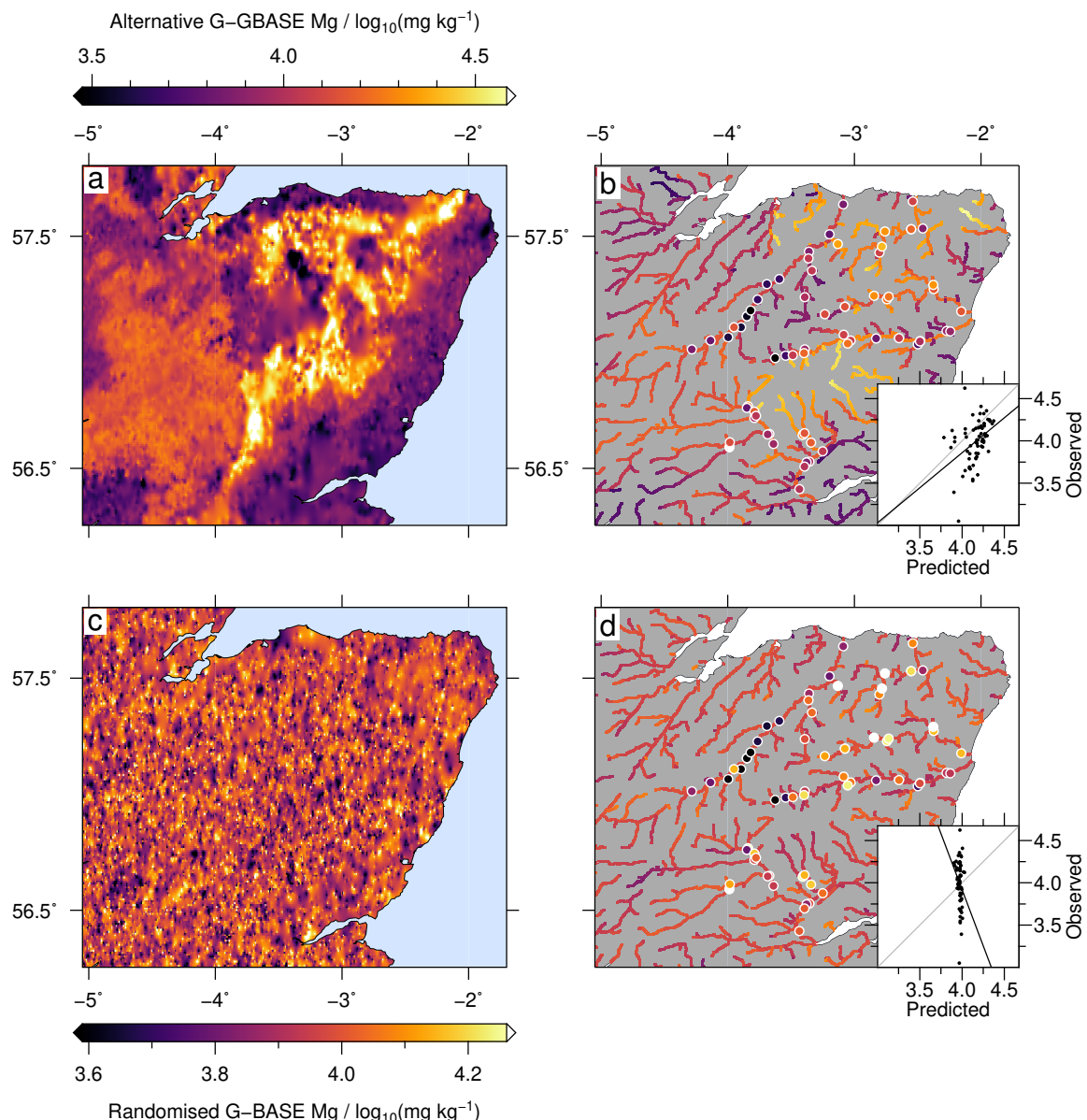


**Figure S1.** Predicted distributions of Mg for different geochemical inputs to the model. (a–b) Predictions generated using an interpolated G-BASE grid taken from elsewhere in UK, here Wales/Herefordshire (panel a). In panel (b) coloured circles = measurements of downstream river chemistry from sampling in this study; drainage patterns are coloured by model predictions; inset graph shows observations compared to predictions (black circles); gray line = 1:1 relationship; black line = best-fitting linear regression. (c–d) Prediction when an interpolated grid generated by randomising the Cairngorms GBASE samples is used as input.

November 18, 2020, 10:21am

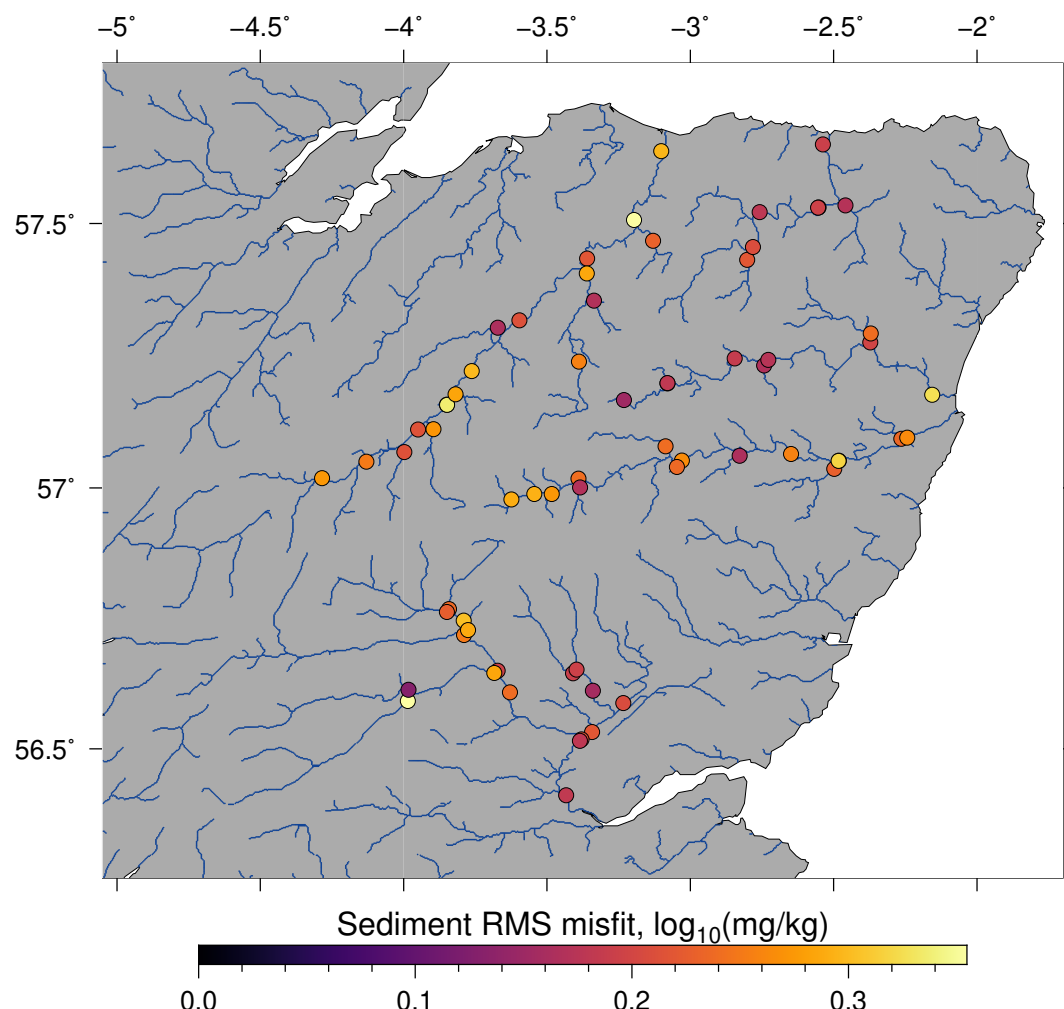


**Figure S2.** Global RMS misfit for all samples in this study.

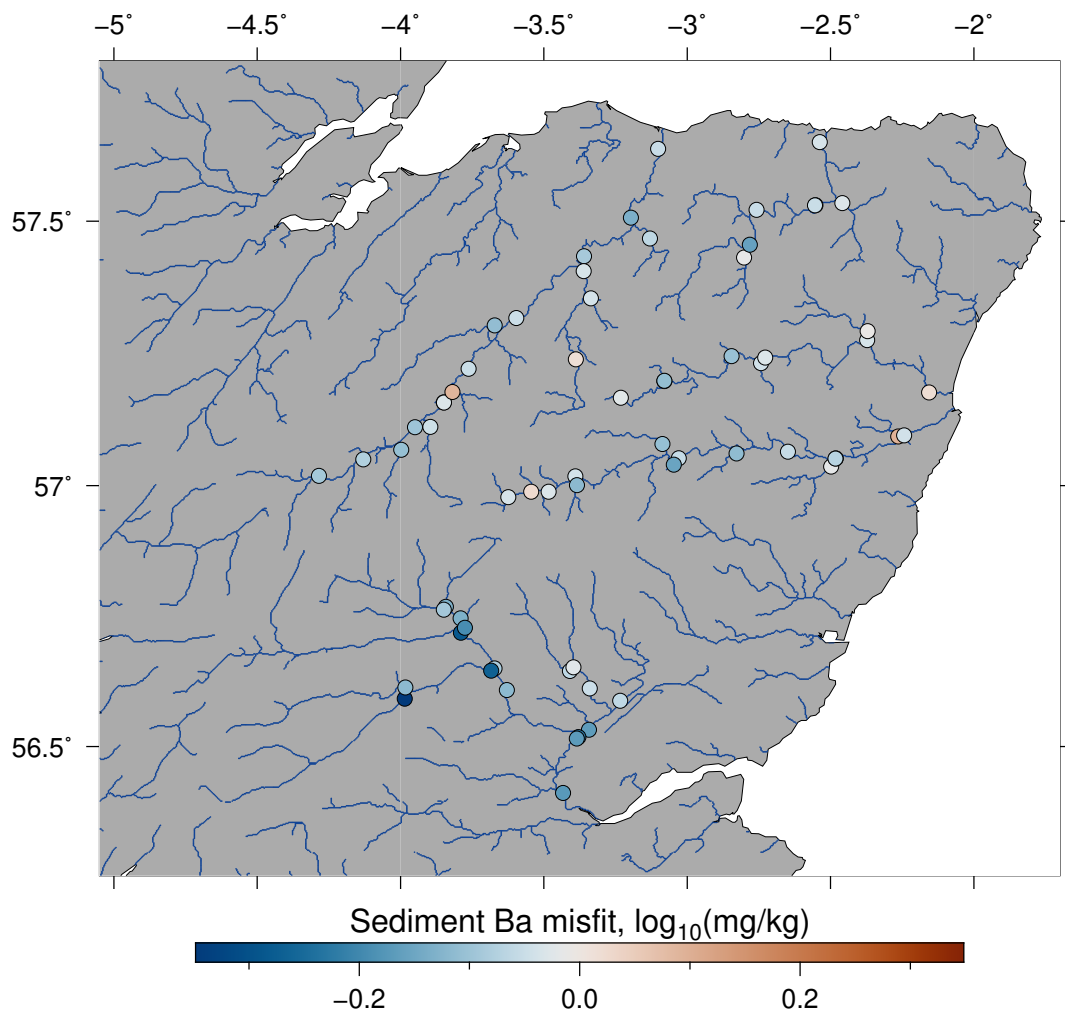


**Figure S3.** Misfit of Ba in bedload chemistry relative to model predictions for all sampled localities

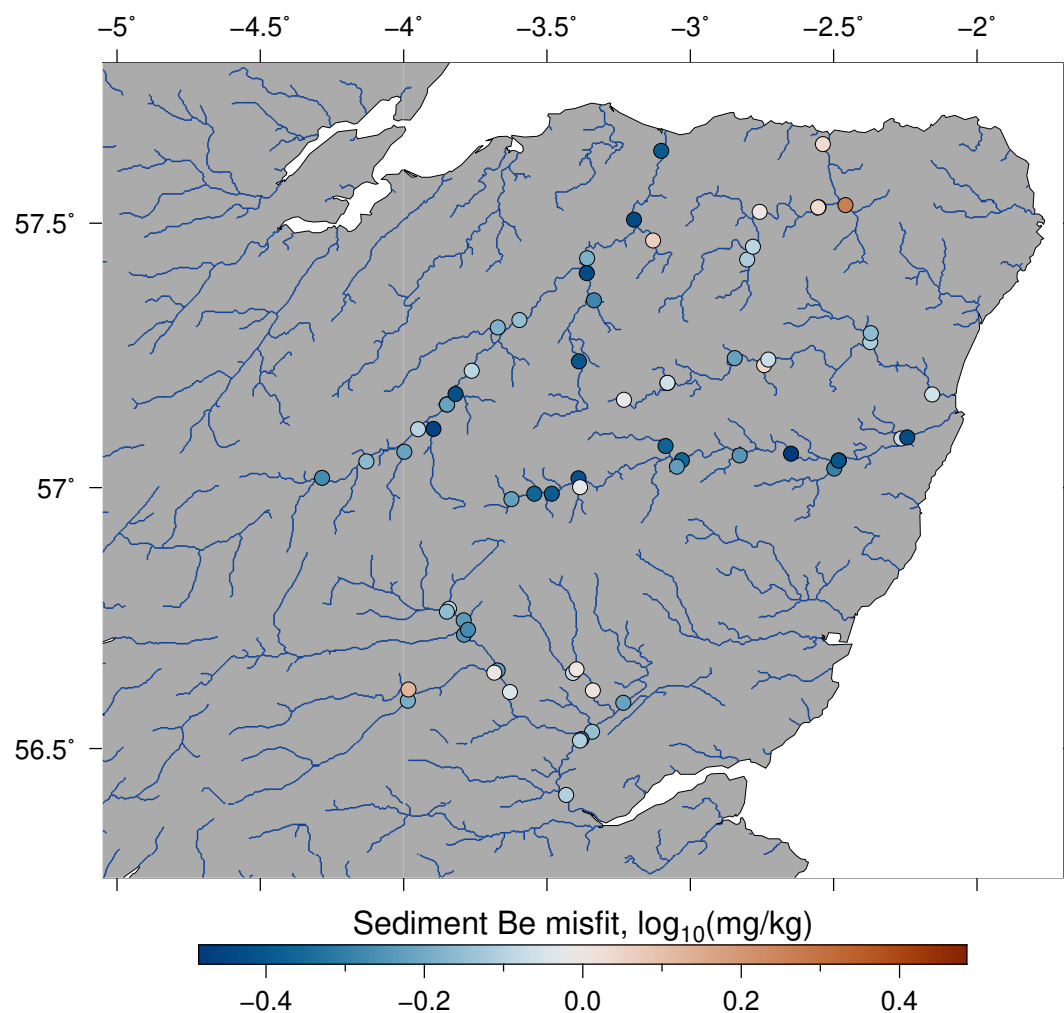


**Figure S4.** Misfit of Be in bedload chemistry relative to model predictions for all sampled localities

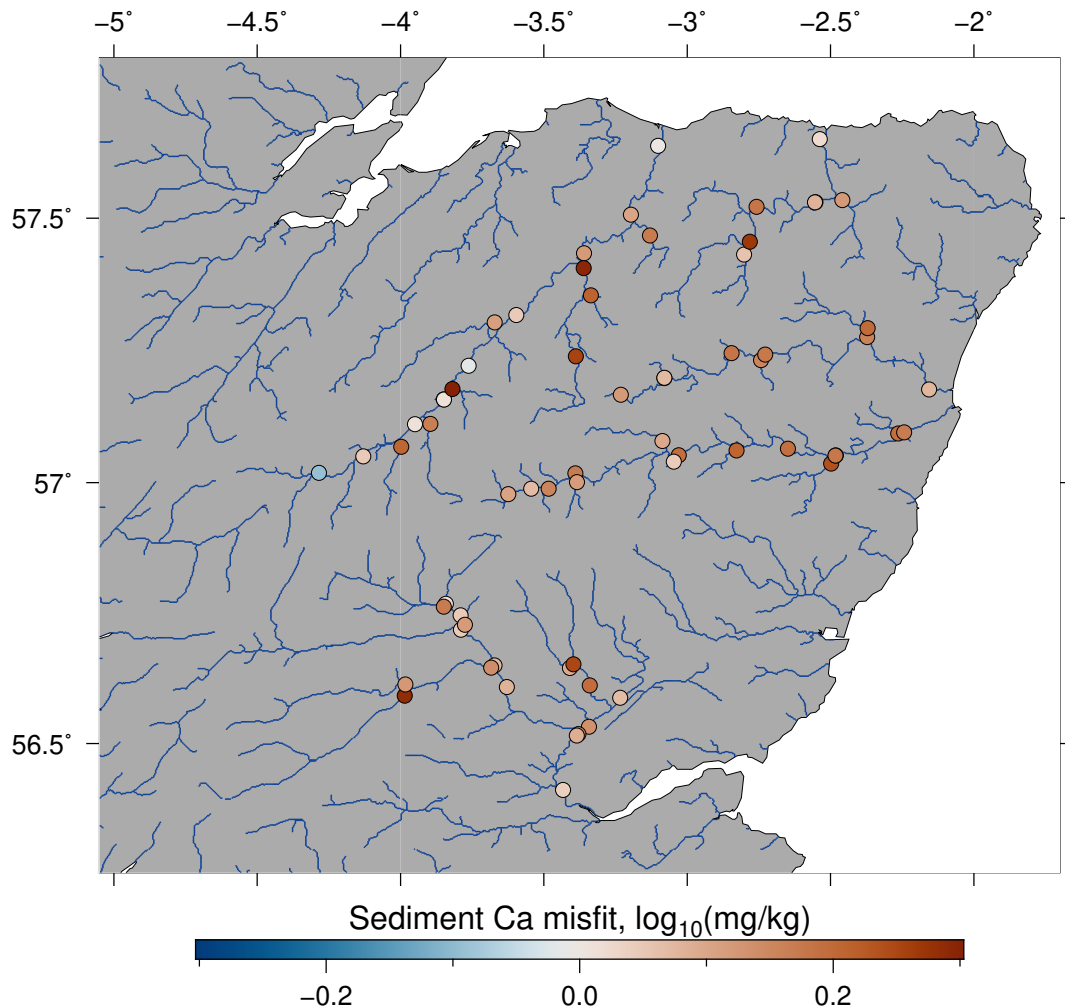


**Figure S5.** Misfit of Ca in bedload chemistry relative to model predictions for all sampled localities

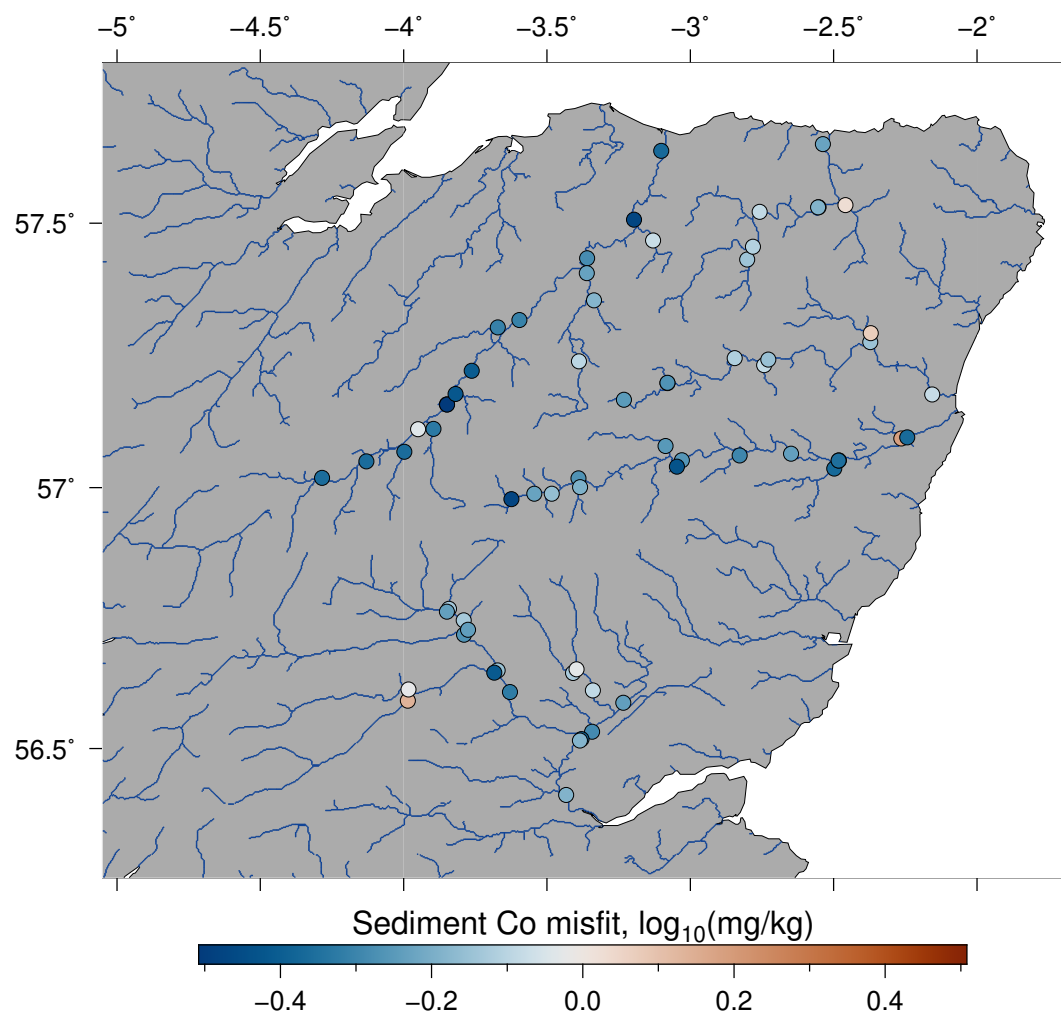


**Figure S6.** Misfit of Co in bedload chemistry relative to model predictions for all sampled localities

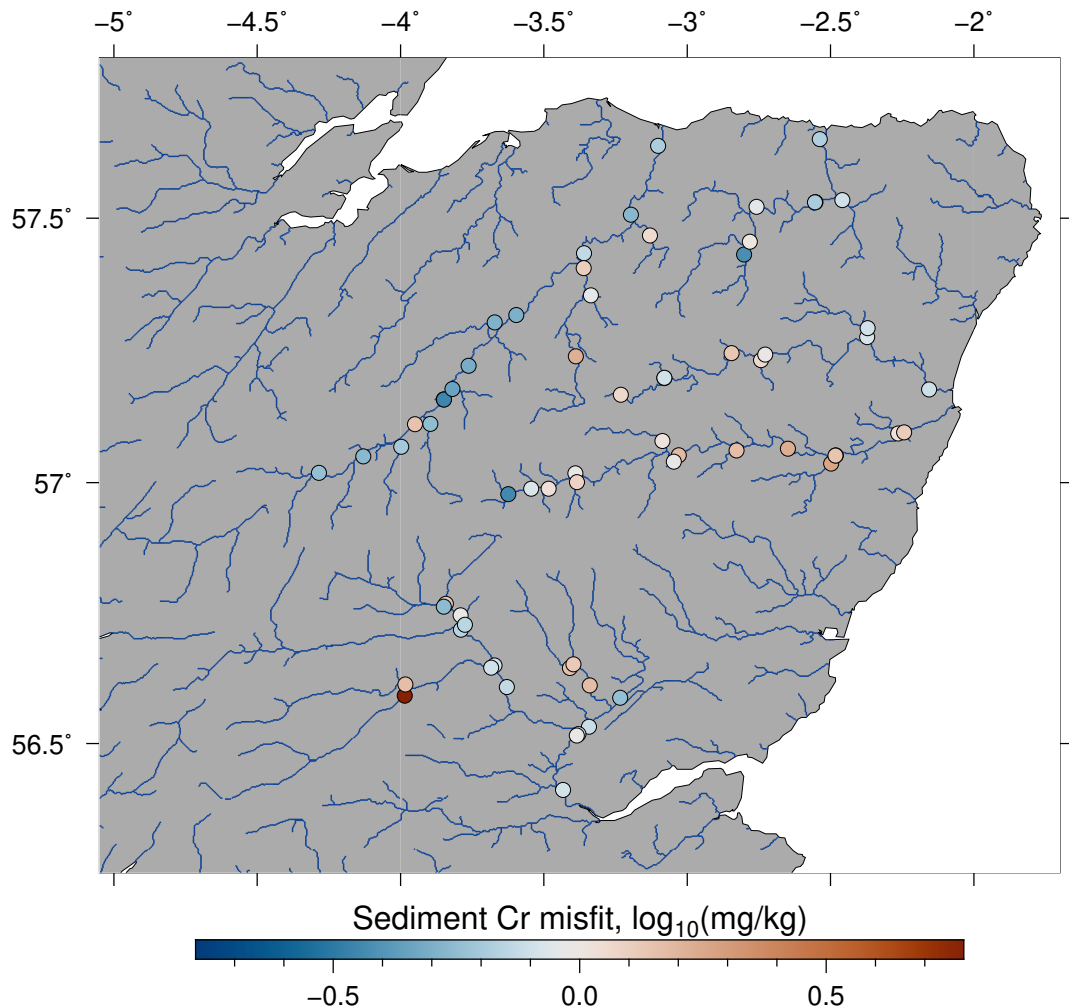


**Figure S7.** Misfit of Cr in bedload chemistry relative to model predictions for all sampled localities

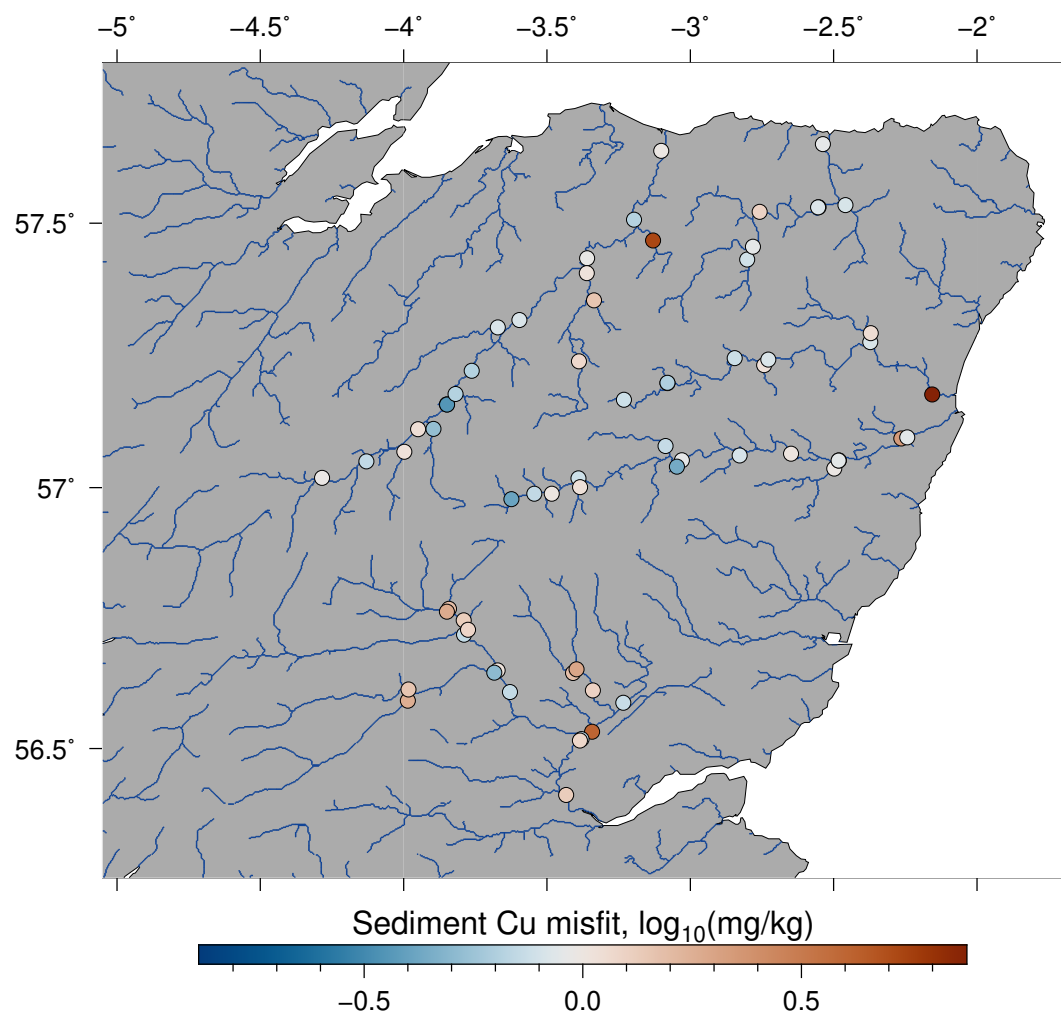


**Figure S8.** Misfit of Cu in bedload chemistry relative to model predictions for all sampled localities

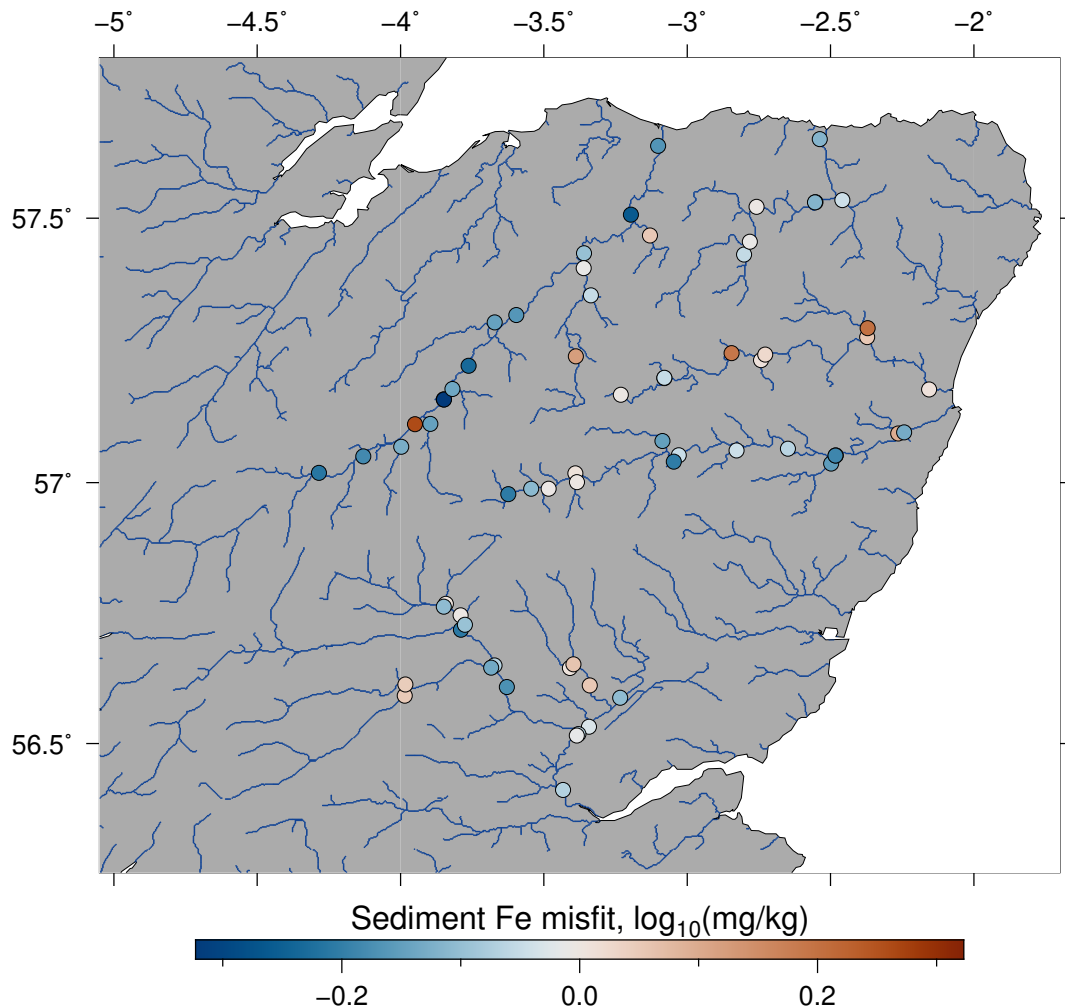


**Figure S9.** Misfit of Fe in bedload chemistry relative to model predictions for all sampled localities

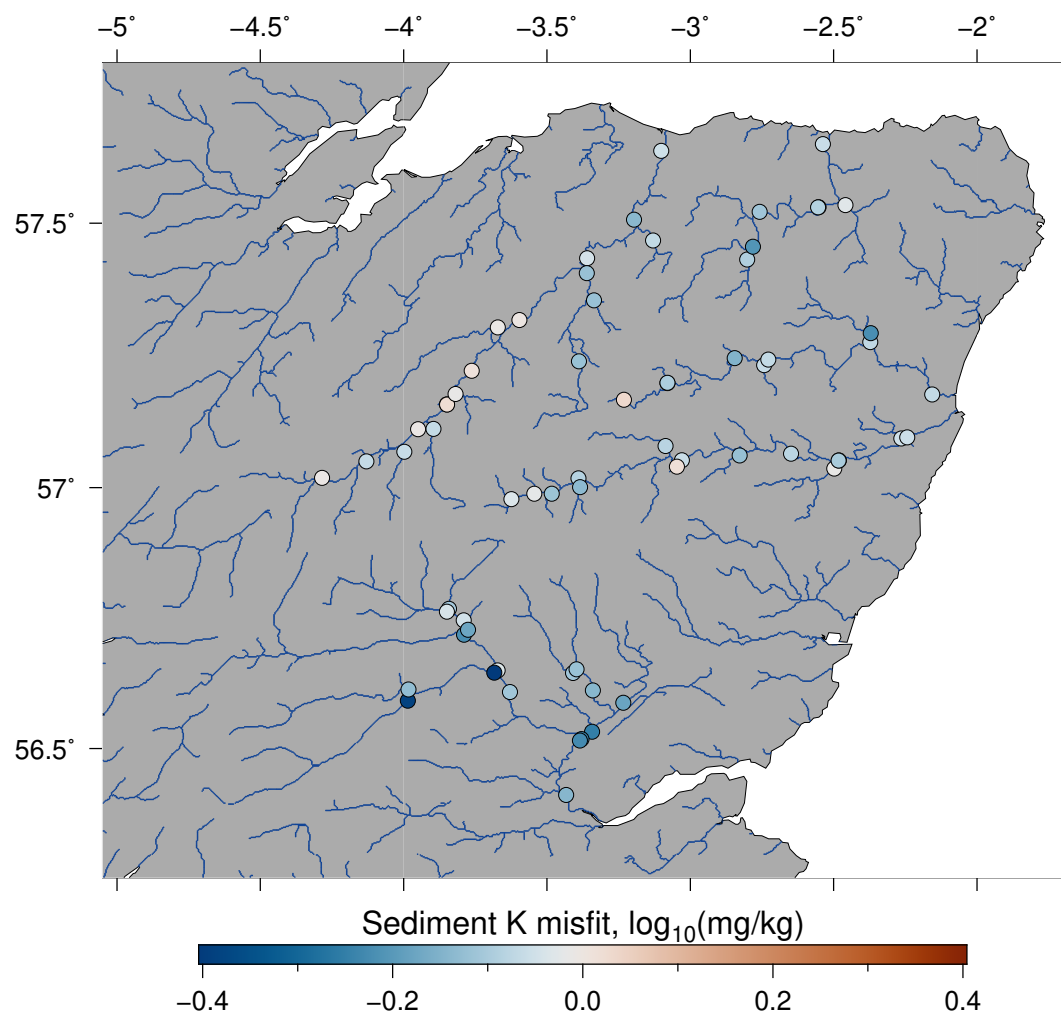


**Figure S10.** Misfit of K in bedload chemistry relative to model predictions for all sampled localities

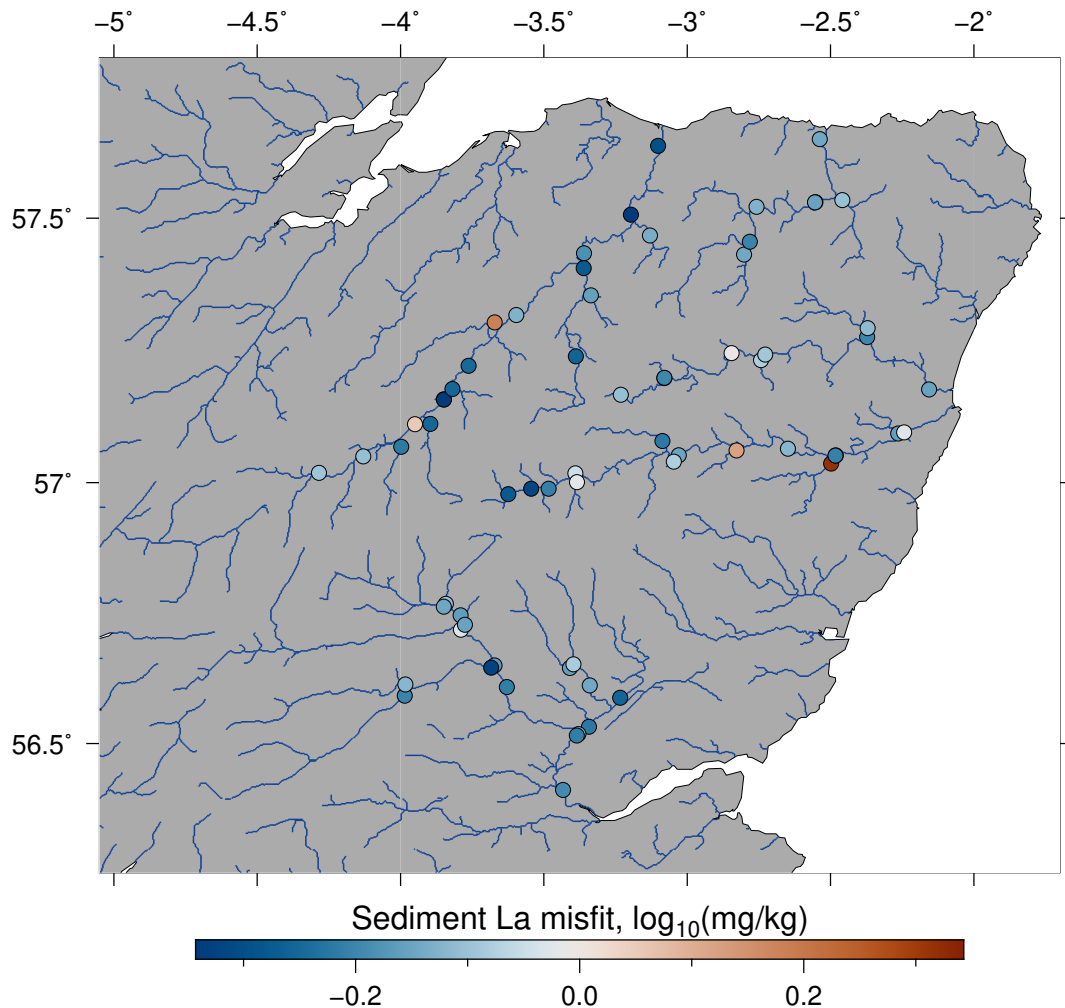


**Figure S11.** Misfit of La in bedload chemistry relative to model predictions for all sampled localities

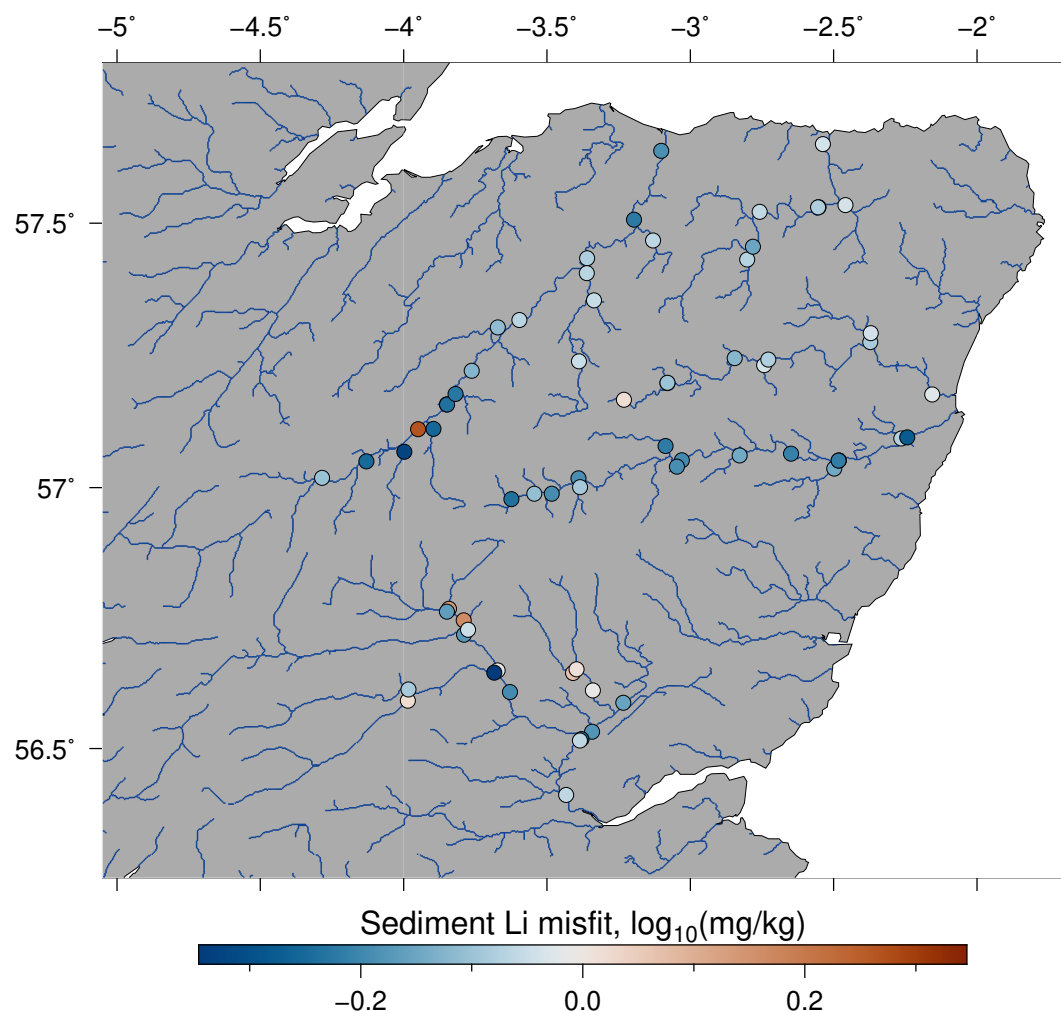


**Figure S12.** Misfit of Li in bedload chemistry relative to model predictions for all sampled localities

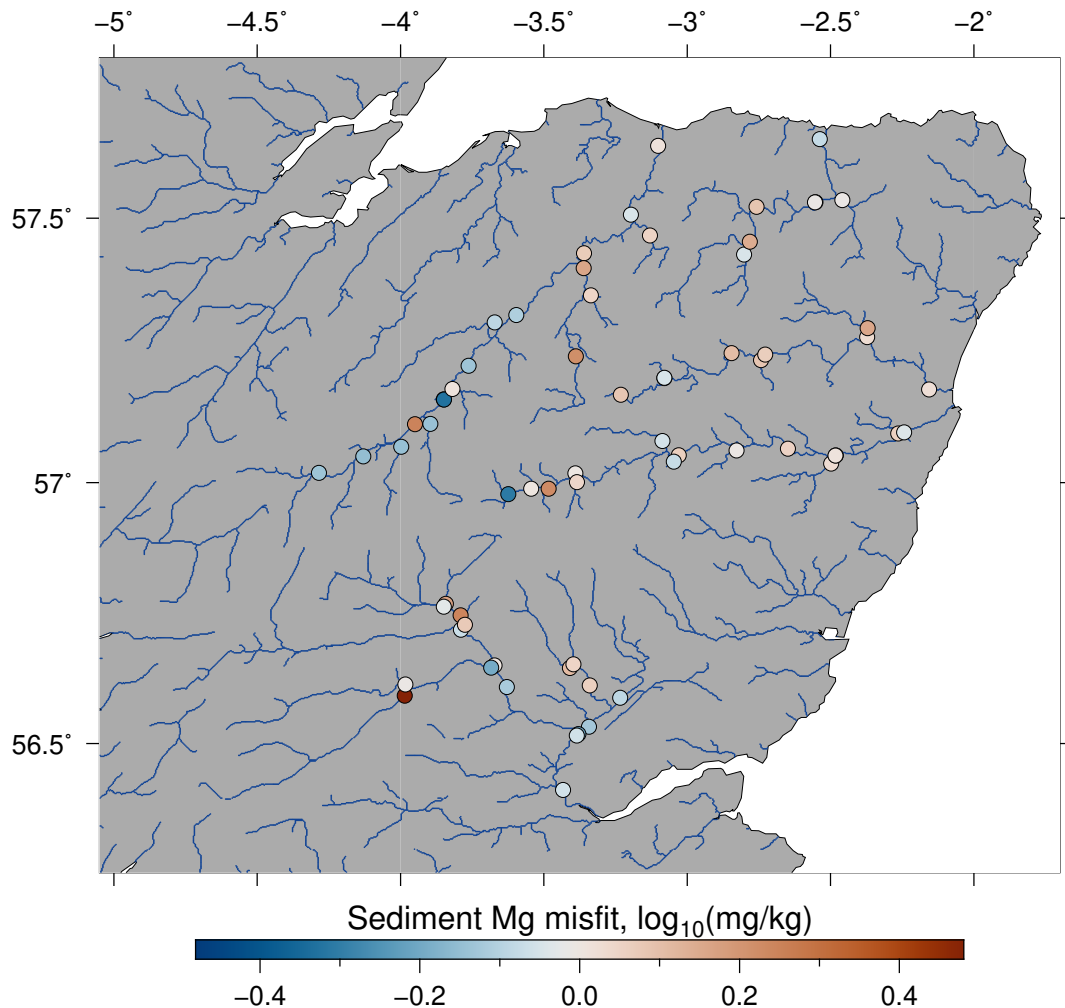


**Figure S13.** Misfit of Mg in bedload chemistry relative to model predictions for all sampled localities

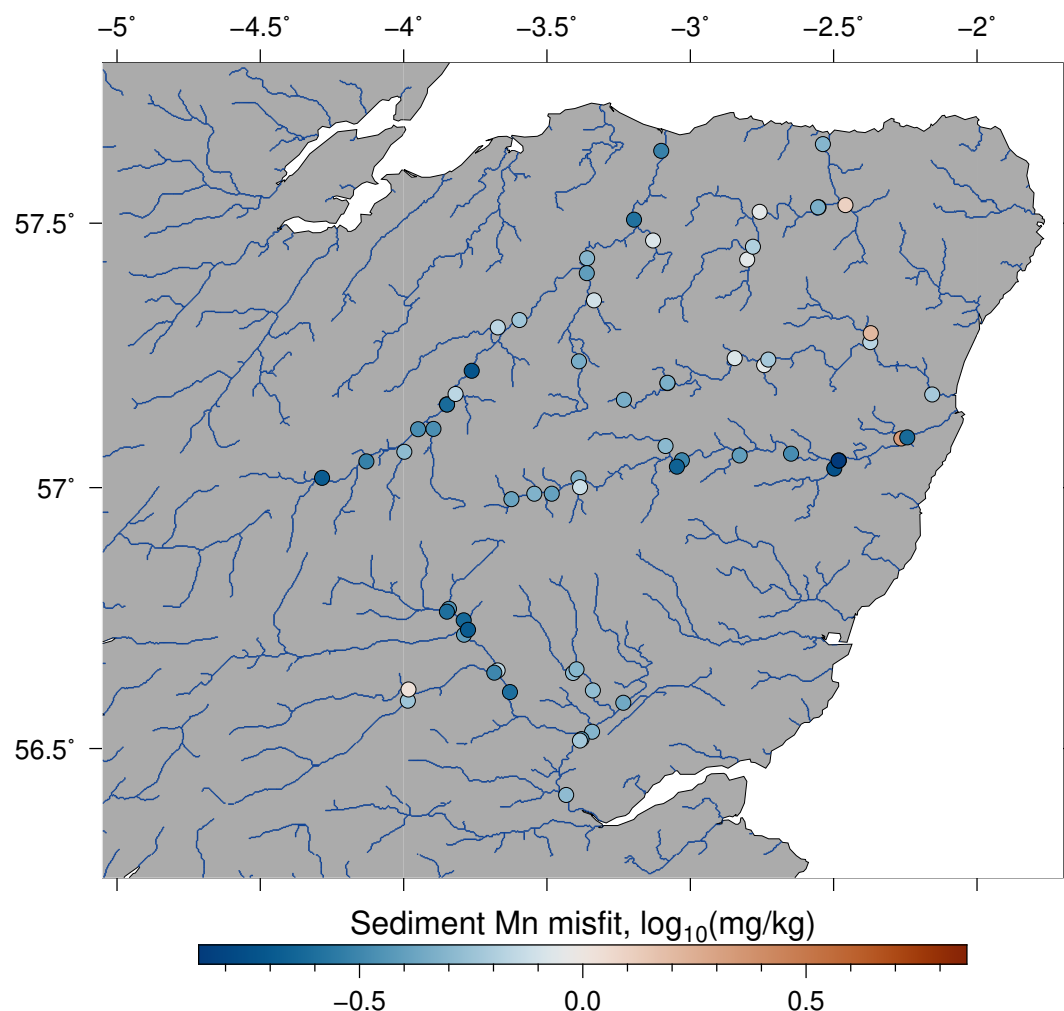


**Figure S14.** Misfit of Mn in bedload chemistry relative to model predictions for all sampled localities

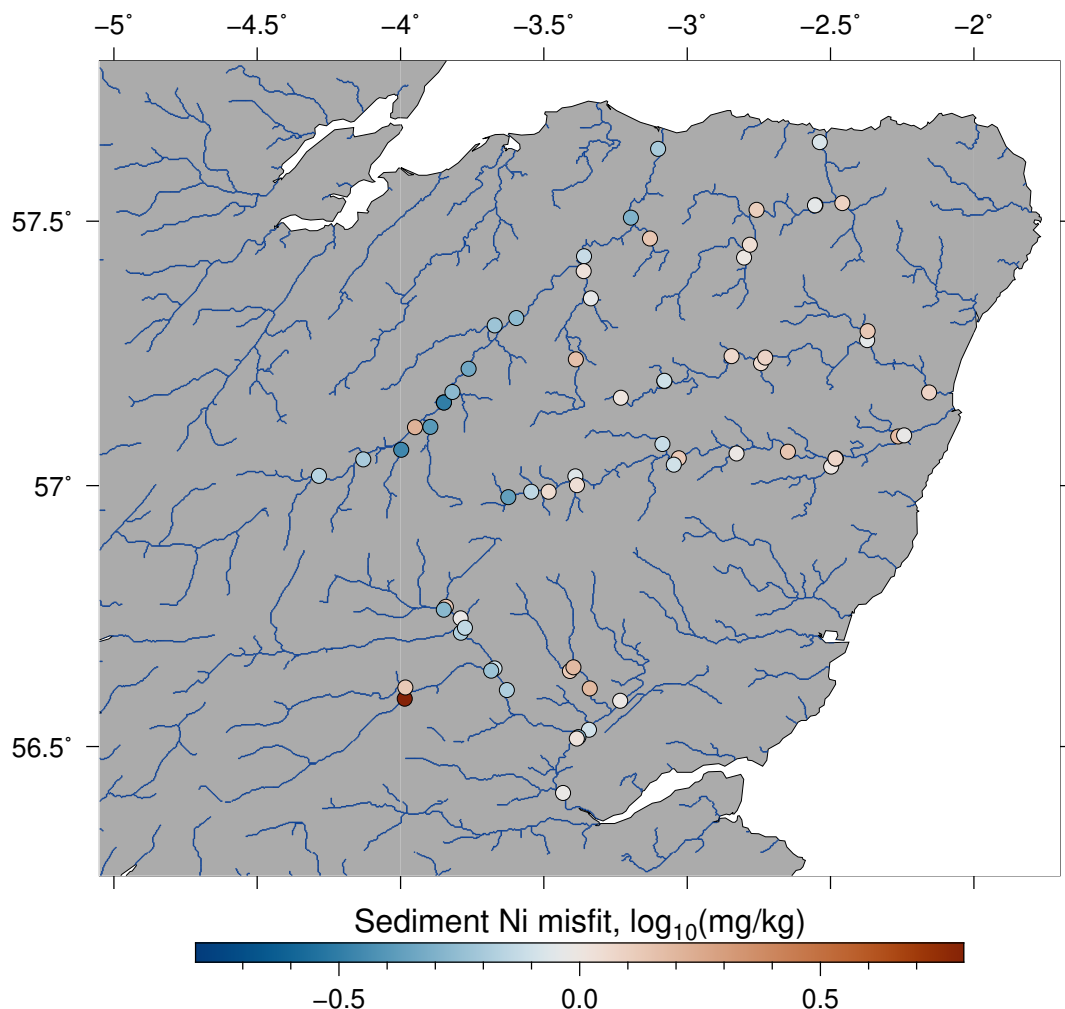


**Figure S15.** Misfit of Ni in bedload chemistry relative to model predictions for all sampled localities

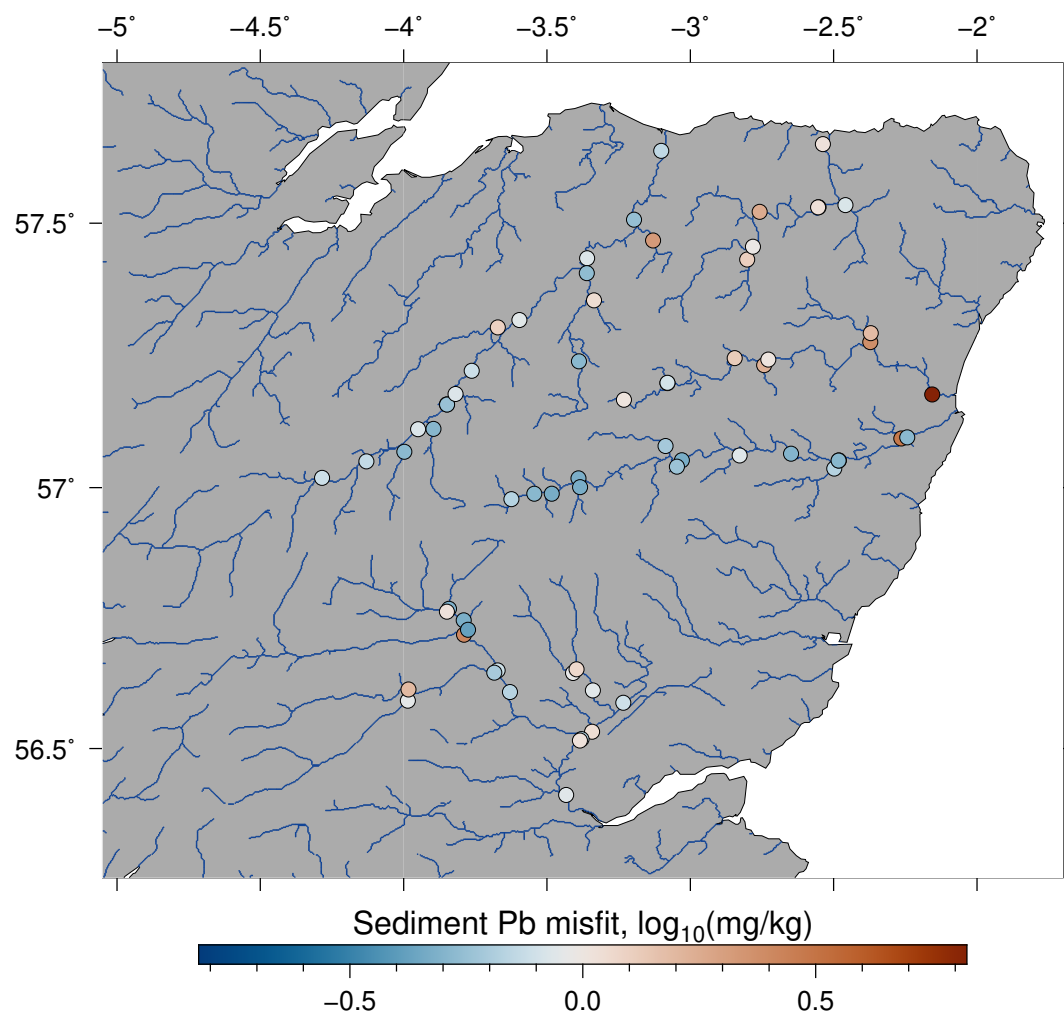


**Figure S16.** Misfit of Pb in bedload chemistry relative to model predictions for all sampled localities

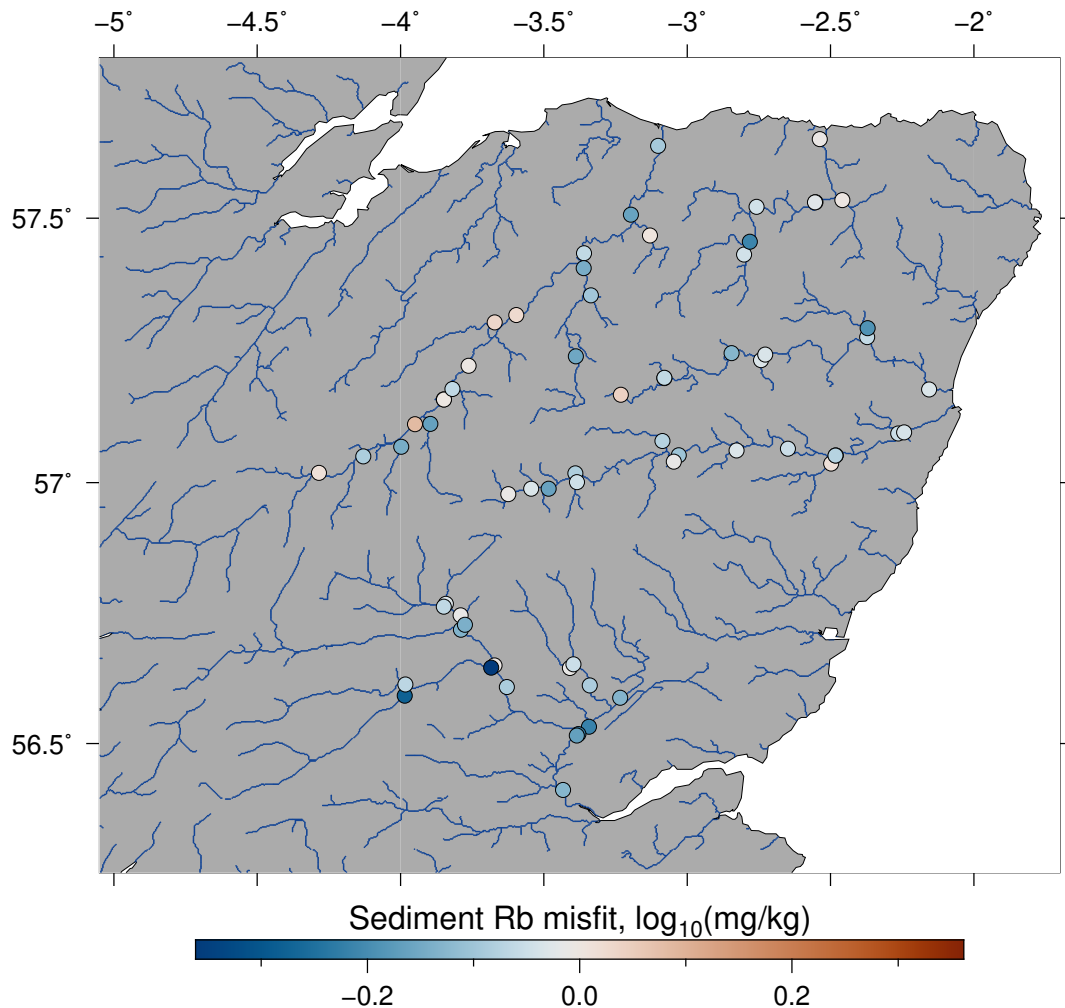


**Figure S17.** Misfit of Rb in bedload chemistry relative to model predictions for all sampled localities

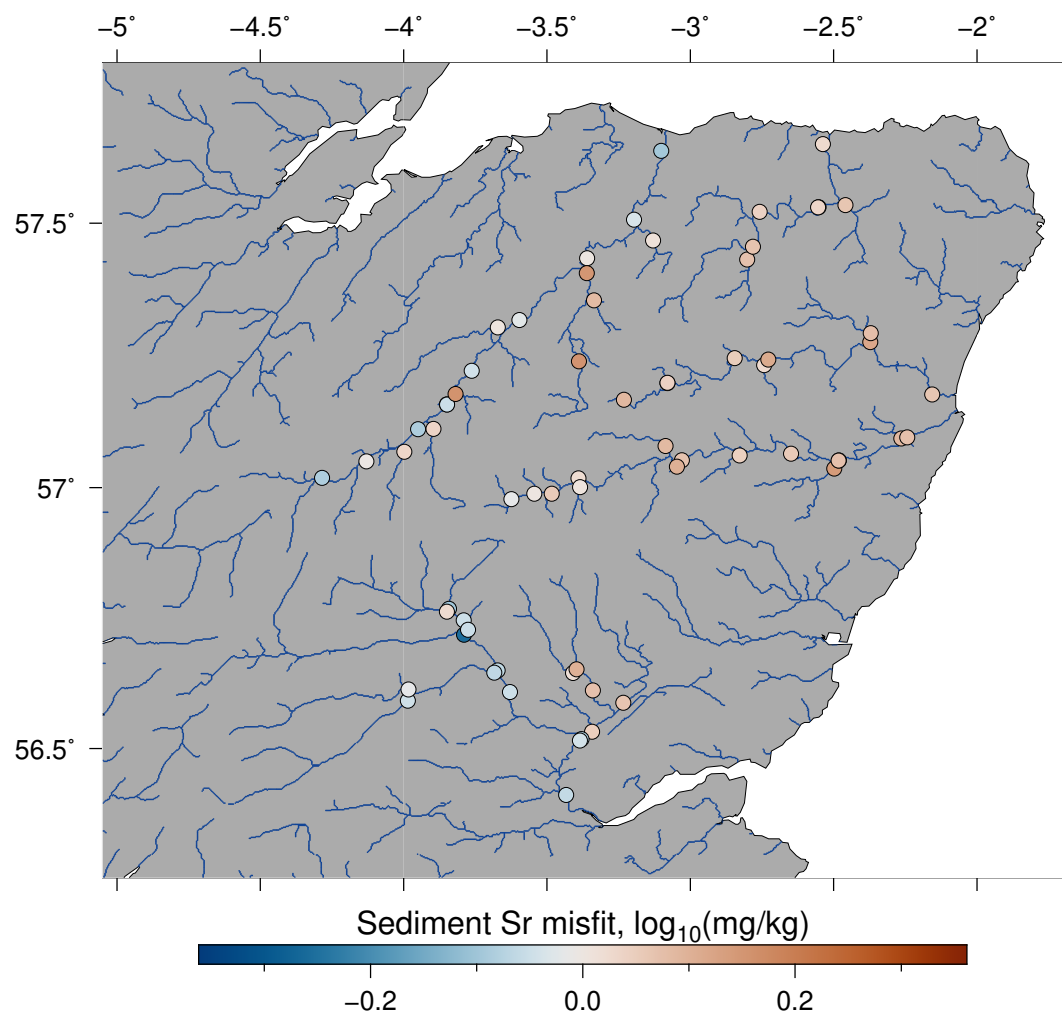


**Figure S18.** Misfit of Sr in bedload chemistry relative to model predictions for all sampled localities

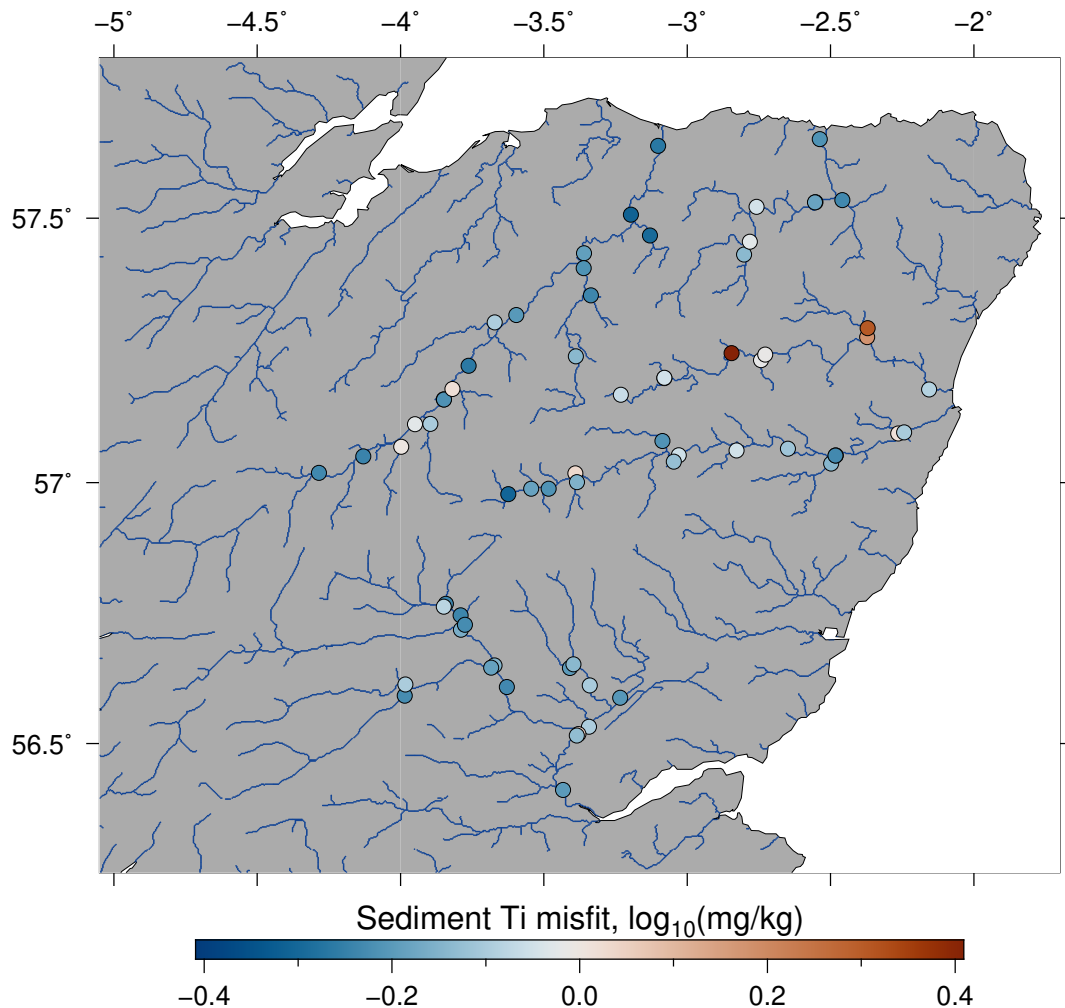


**Figure S19.** Misfit of Ti in bedload chemistry relative to model predictions for all sampled localities

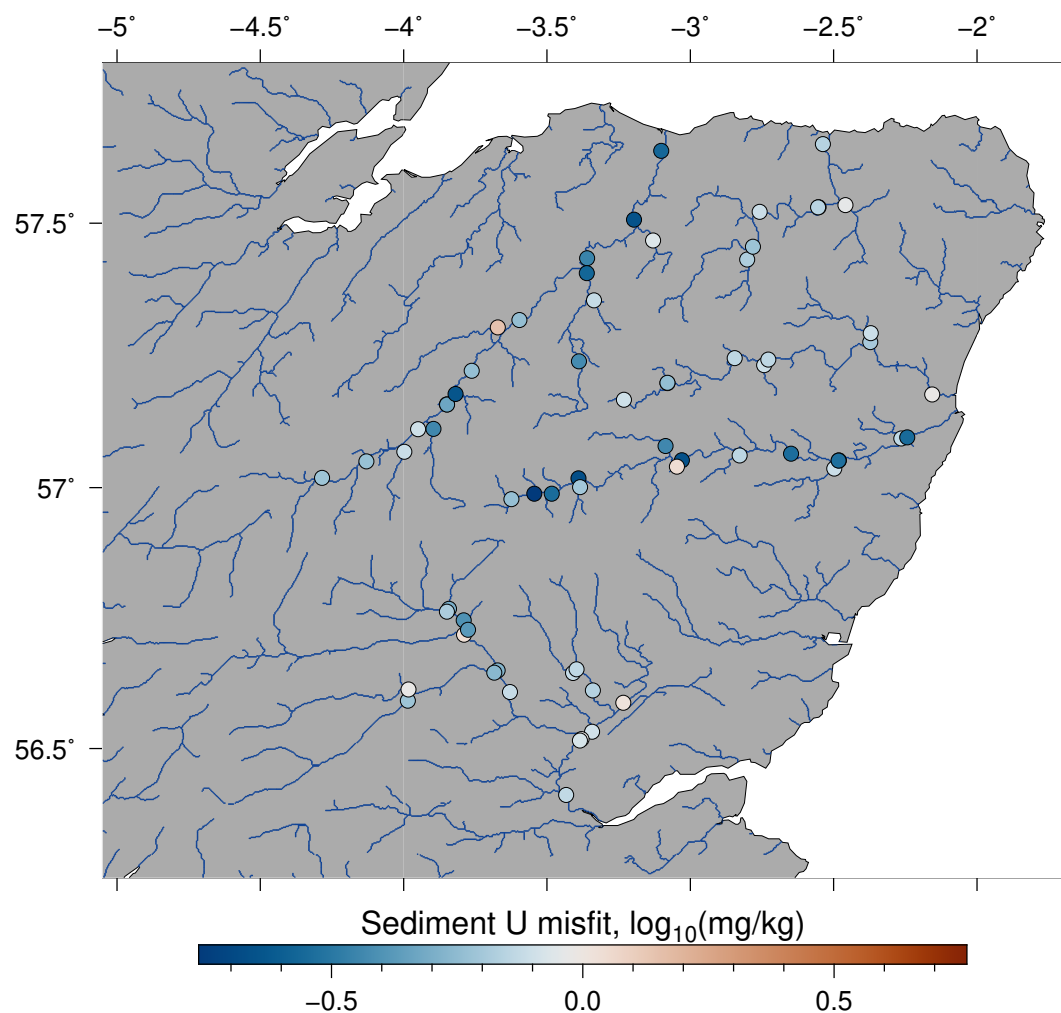


**Figure S20.** Misfit of U in bedload chemistry relative to model predictions for all sampled localities

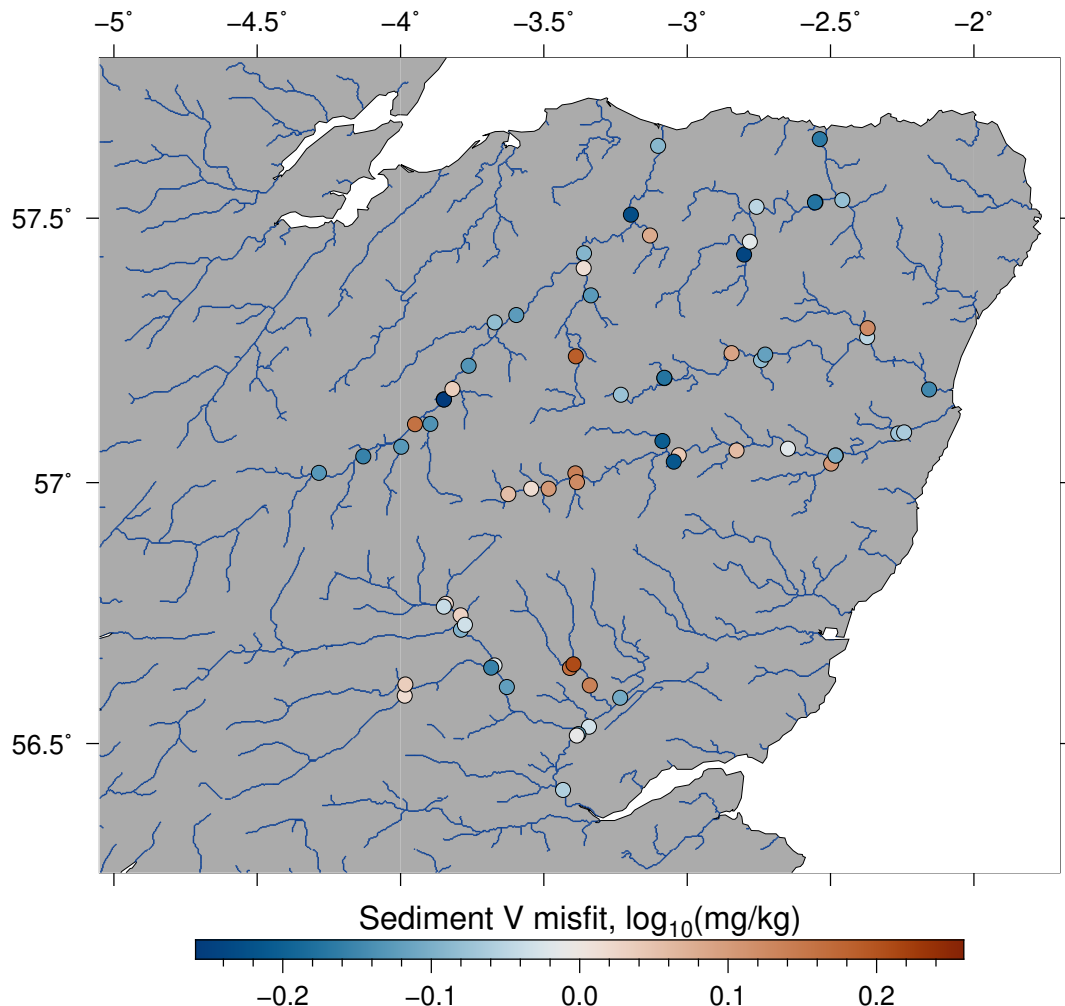


**Figure S21.** Misfit of V in bedload chemistry relative to model predictions for all sampled localities

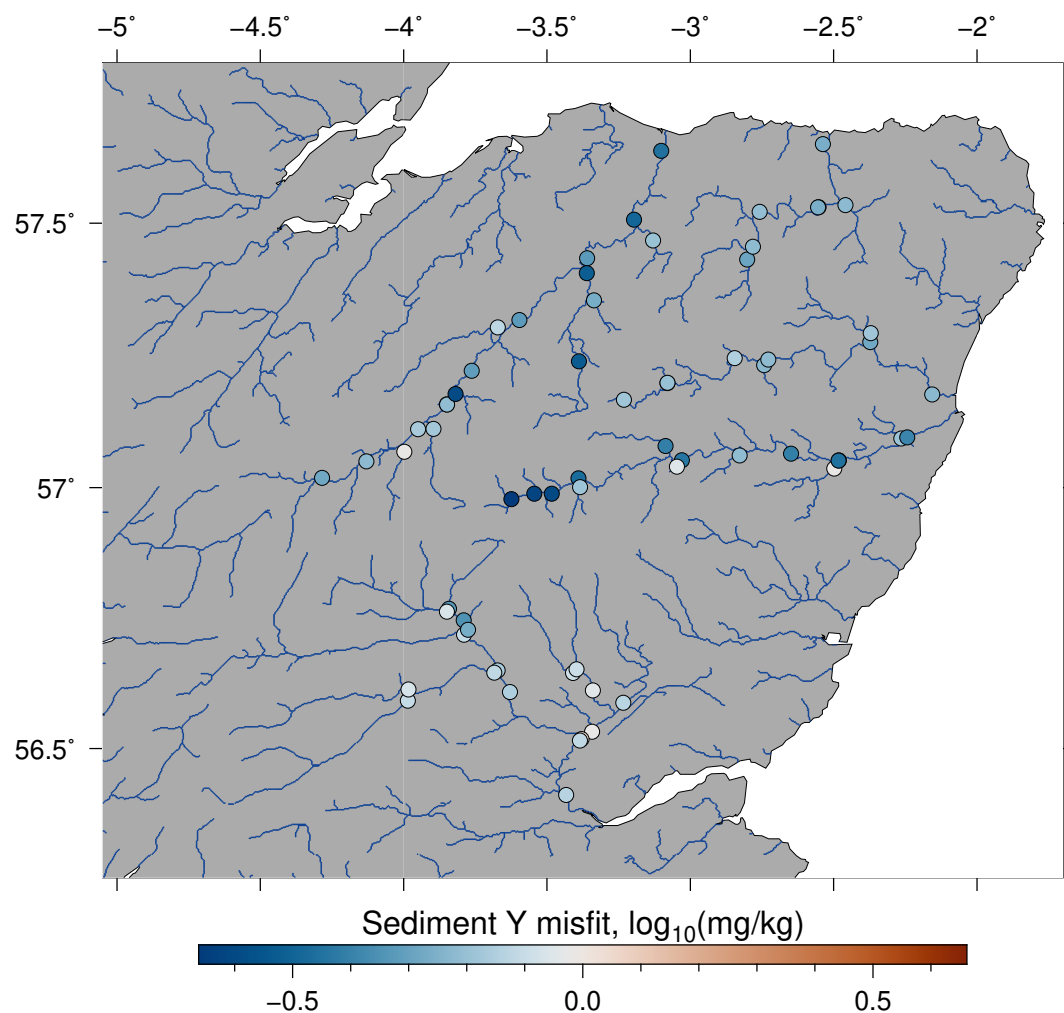


**Figure S22.** Misfit of Y in bedload chemistry relative to model predictions for all sampled localities

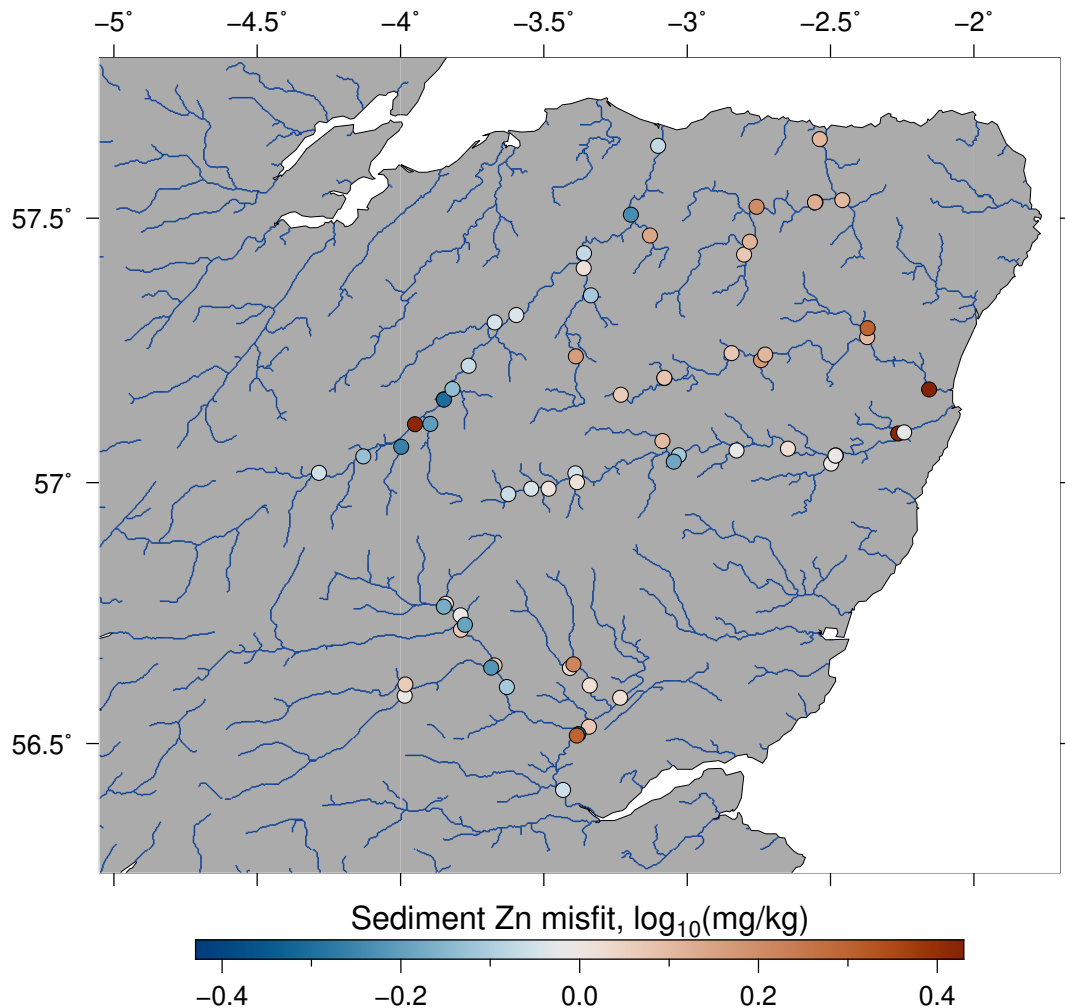


**Figure S23.** Misfit of Zn in bedload chemistry relative to model predictions for all sampled localities

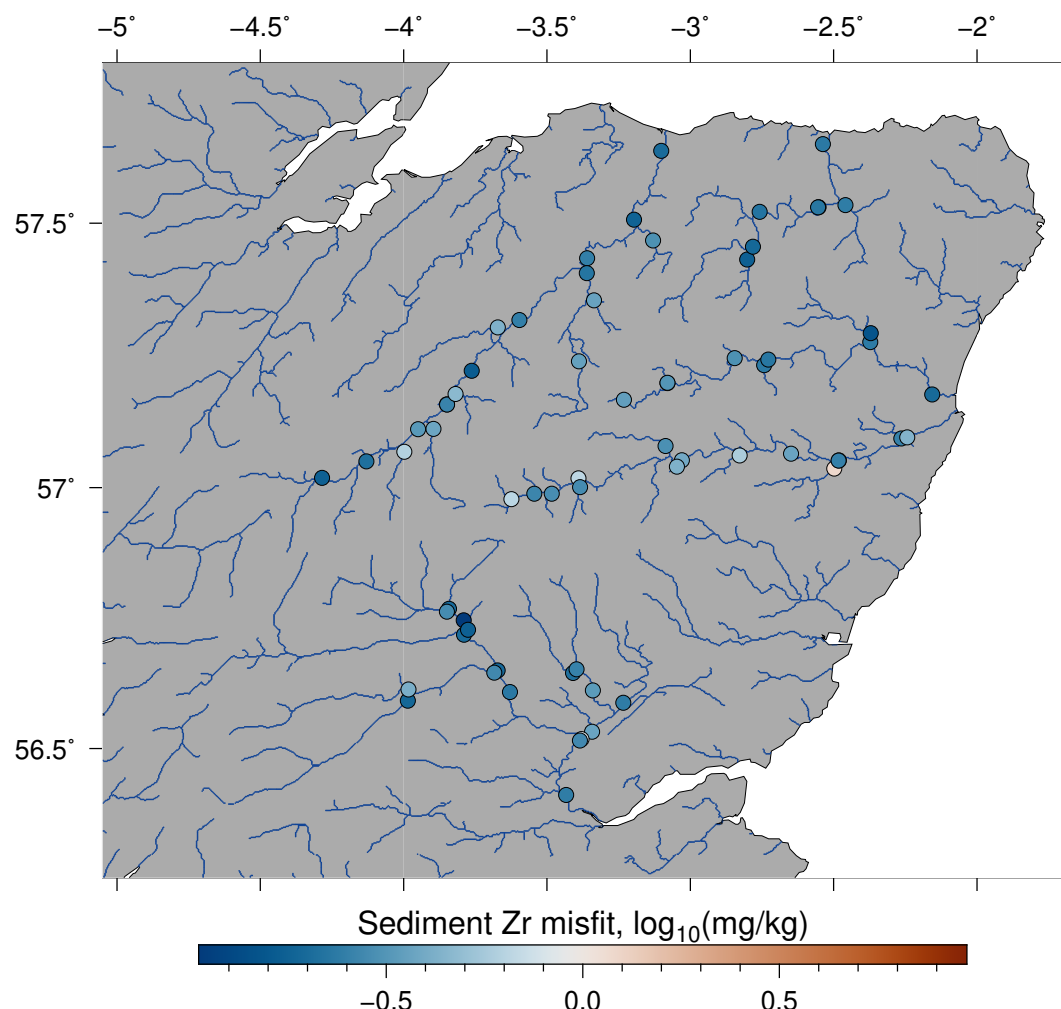


**Figure S24.** Misfit of Zr in bedload chemistry relative to model predictions for all sampled localities